SIAM J. SCI. COMPUT.
Vol. 37, No. 6, pp. A2607–A2629

COMPUTING THE EIGENVALUES OF REALISTIC DAPHNIA MODELS BY PSEUDOSPECTRAL METHODS*

D. BREDA†, P. GETTO‡, J. SÁNCHEZ SANZ§, AND R. VERMIGLIO†

Abstract. This work deals with physiologically structured populations of the Daphnia type. Their biological modeling poses several computational challenges. In such models, indeed, the evolution of a size structured consumer described by a Volterra functional equation (VFE) is coupled to the evolution of an unstructured resource described by a delay differential equation (DDE), resulting in dynamics over an infinite dimensional state space. As additional complexities, the right-hand sides are both of integral type (continuous age distribution) and given implicitly through external ordinary differential equations (ODEs). Moreover, discontinuities in the vital rates occur at a maturation age, also given implicitly through one of the above ODEs. With the aim at studying the local asymptotic stability of equilibria and relevant bifurcations, we revisit a pseudospectral approach recently proposed to compute the eigenvalues of the infinitesimal generator of linearized systems of coupled VFEs/DDEs. First, we modify it in view of extension to nonlinear problems for future developments. Then, we consider a suitable implementation to tackle all the computational difficulties mentioned above: a piecewise approach to handle discontinuities, numerical quadrature of integrals, and numerical solution of ODEs. Moreover, we rigorously prove the spectral accuracy of the method in approximating the eigenvalues and how this outstanding feature is influenced by the other unavoidable error sources. Implementation details and experimental computations on existing available data conclude the work.

Key words. physiologically structured populations, Volterra functional equations, delay differential equations, numerical equilibrium analysis, pseudospectral methods

AMS subject classifications. 34L16, 34K06, 37M20, 65L07, 92D25

DOI. 10.1137/15M1016710

1. Introduction.

We propose a numerical technique to study the local stability of equilibria of physiologically structured populations of the Daphnia type. This rather long introduction serves to describe the model (section 1.1), to motivate our proposal (end of section 1.2), and to illustrate the new contributions (end of section 1.3). In section 2 we present the numerical method and prove its convergence. In section 3 we discuss the necessary variants and implementation details to tackle the computational difficulties posed by the biological modeling itself. In section 4 we test the proposed scheme confirming the theoretical results and experimenting on existing data.

*Submitted to the journal's Methods and Algorithms for Scientific Computing section April 13, 2015; accepted for publication (in revised form) September 18, 2015; published electronically November 10, 2015.

http://www.siam.org/journals/sisc/37-6/M101671.html

†Department of Mathematics and Computer Science, University of Udine, via delle scienze 206, I-33100 Udine, Italy (dimitri.breda@uniud.it, rossana.vermiglio@uniud.it). These authors were supported by the Italian National Scientific Computing Group 2014 grant "Numerical analysis of infinite-dimensional and discontinuous differential problems."

‡Fachrichtung Mathematik, Institut für Analysis, TU Dresden, 01062 Dresden, Germany, and BCAM–Basque Center for Applied Mathematics, Alameda de Mazarredo 14, E-48009 Bilbao, Bizkaia, Spain (Philipp.Getto@tu-dresden.de, phgetto@yahoo.com). The research of this author is part of the "Delay equations and structured population dynamics" project funded by DFG (Deutsche Forschungsgemeinschaft). Additional support is by MINECO (Spain) under project MTM 2010-18318.

§BCAM–Basque Center for Applied Mathematics, Alameda de Mazarredo 14, E-48009 Bilbao, Bizkaia, Spain (jsanchez@bcamath.org). This author was supported by MINECO (Spain) through FPI grant BES-2011-047867, projects MTM2010-18318 and MTM2013-46553-C3-1-P, internship EEBB-I-2014-08194, and Severo Ochoa Excellence accreditation SEV-2013-0323.

1.1. Daphnia models. We consider a size structured consumer population competing for an unstructured resource. Here we summarize the basic features of the model commonly called *Daphnia consuming algae* and described in detail, e.g., in [16]. See also [10, 11, 12, 13, 14, 17] for a broad literature review and the background results of interest for this work.

By $S(t) \in [0, +\infty)$ we denote the available resource concentration at time t. In absence of consumers, its evolution in time is determined by the ODE Cauchy problem

$$\begin{cases} S'(t) = f(S(t)), & t \geq 0, \\ S(0) = S_0, \end{cases} \tag{1.1}$$

for a given f. The history of the resource at time t is given by the function $S_t : [-h, 0] \to [0, +\infty)$ for some $h > 0$, defined as the shift $S_t(\theta) := S(t+\theta)$ for $\theta \in [-h, 0]$. Histories are commonly used in the theory of delay equations [18, 22, 23, 30].

By $X(a, S_t) \in [0, +\infty)$ we denote the body size of a consumer individual that at time t has age a and has experienced a resource history S_t during its life. The size of an individual changes w.r.t. its age, depending on a given growth rate g. The size at age α of an individual that at age a has experienced a resource history ψ, say, $x(\alpha) := x(\alpha; a, \psi)$ for $0 \leq \alpha \leq a$, is determined through the ODE Cauchy problem

$$\begin{cases} x'(\alpha) = g(x(\alpha), \psi(-a + \alpha)), & 0 \leq \alpha \leq a, \\ x(0) = x_b, \end{cases} \tag{1.2}$$

for x_b a given size at birth. Then, the size at age a is given by $X(a, \psi) = x(a; a, \psi)$.

In the same way, by $\mathcal{F}(a, S_t) \in [0, 1]$ we denote the survival probability of a consumer individual that at time t has age a and has experienced a resource history S_t during its life. The survival probability of an individual decreases w.r.t. its age, depending on a given positive mortality rate μ. The survival probability at age α of an individual that at age a has experienced a resource history ψ, say, $\bar{\mathcal{F}}(\alpha) := \bar{\mathcal{F}}(\alpha; a, \psi)$ for $0 \leq \alpha \leq a$, is determined through the ODE Cauchy problem

$$\begin{cases} \bar{\mathcal{F}}'(\alpha) = -\mu(x(\alpha), \psi(-a + \alpha))\bar{\mathcal{F}}(\alpha), & 0 \leq \alpha \leq a, \\ \bar{\mathcal{F}}(0) = 1. \end{cases} \tag{1.3}$$

Then, the survival probability at age a is given by $\mathcal{F}(a, \psi) = \bar{\mathcal{F}}(a; a, \psi)$.

The reproduction rate of a consumer individual that at time t has age a and size $X(a, S_t)$ is denoted by $\beta(X(a, S_t), S(t))$ for a given β. Similarly, its ingestion rate is denoted by $\gamma(X(a, S_t), S(t))$ for a given γ.

We assume two life stages for the consumers: juveniles and adults. The individuals are juveniles from birth until they reach a given maturation size x_A. During the juvenile period they are not able to produce offspring, hence we assume $\beta(x, y) = 0$ for $x_b \leq x < x_A$. When the individuals reach size x_A, they become adults and are able to reproduce. We denote by $a_A(\psi)$ the age at which a consumer reaches size x_A under resource history ψ, that is,

$$X(a_A(\psi), \psi) = x_A.$$

Correspondingly, the rates β, g, γ, and μ are assumed to be functions sufficiently piecewise smooth on $[x_b, x_A] \times [0, +\infty)$ and on $[x_A, +\infty) \times [0, +\infty)$. On the other hand, the function f in (1.1) is assumed to be sufficiently smooth on $[0, +\infty)$. Notice that the sufficient degree of smoothness assumed in [16] is C^1, whereas, as discussed in section 3, the one assumed in this work is as high as needed for numerical purposes.

The dynamics at the population level is modeled as a system of a Volterra functional equation (VFE) coupled to a delay differential equation (DDE). Let us denote by $b(t)$ the consumer birth rate at time t. The number of individuals that at time t have age a is equal to the number of individuals that were born at time $t-a$ and had survived till age a, i.e., $\mathcal{F}(a, S_t)b(t-a)$. Then, the population birth rate at time t is obtained by integrating w.r.t. the age the contribution to the birth rate of the individuals that have age a at time t:

$$b(t) = \int_{a_A(S_t)}^{h} \beta(X(a, S_t), S(t))\mathcal{F}(a, S_t)b(t-a)da. \tag{1.4}$$

Here h is a given maximum age that an individual can reach. In the same way, we obtain the population total ingestion of food by integrating the contribution of the individual food consumption rate. Then, we get the evolution in time of the resource by subtracting the total ingestion from the right-hand side of (1.1):

$$S'(t) = f(S(t)) - \int_0^h \gamma(X(a, S_t), S(t))\mathcal{F}(a, S_t)b(t-a)da. \tag{1.5}$$

We complete the system (1.4)–(1.5) with initial histories $b(\theta) = \phi(\theta)$ and $S(\theta) = \psi(\theta)$, $\theta \in [-h, 0]$, for given $\phi \in L_1([-h, 0]; \mathbb{R})$ and $\psi \in C([-h, 0]; \mathbb{R})$, as motivated in [14].

1.2. Local stability of equilibria. An equilibrium for (1.4)–(1.5) is a pair of constants $(\bar{b}, \bar{S})$ (such that) $b(t) = \bar{b}$ and $S(t) = \bar{S}$ for all $t \geq 0$. By introducing the functions

$$R_0(\bar{S}) := \int_{\bar{a}_A}^{h} \beta(X(a, \bar{S}), \bar{S})\mathcal{F}(a, \bar{S})da, \qquad \Theta(\bar{S}) := \int_0^h \gamma(X(a, \bar{S}), \bar{S})\mathcal{F}(a, \bar{S})da$$

from [11] for $\bar{a}_A := a_A(\bar{S})$, it is not difficult to see that (1.4)–(1.5) has a trivial equilibrium $(0, \bar{S})$ iff $\bar{S}$ satisfies $f(\bar{S}) = 0$ and a positive equilibrium $(\bar{b}, \bar{S})$ iff $\bar{b}$ and $\bar{S}$ are positive constants satisfying $1 - R_0(\bar{S}) = 0$ and $f(\bar{S}) - \bar{b}\Theta(\bar{S}) = 0$.

The Daphnia model under study is an example of a system of VFEs/DDEs; see [16]. The principle of linearized stability for VFEs/DDEs is shown in [14]. For a constructive approach toward verification of differentiability conditions when discontinuities come into play see [17]. This principle relies on the linearization around the equilibrium. The latter for (1.4)–(1.5) with (1.2)–(1.3) is performed in [16, sections 3 and 4] and in [11, Appendix A]. It involves differentiation of $a_A(\psi)$, $X(a, \psi)$, and $\mathcal{F}(a, \psi)$ w.r.t. ψ. These functions are only implicitly defined via (1.2)–(1.3). Additional complications arise from possible discontinuities at the right-hand side of both equations.

In the process of elaborating on the results in [16, section 4] we found that the formula [16, (4.22)] for $D_3x(\tau; a, \bar{S})\psi$ is incorrect (one way of seeing this is that it does not satisfy the linearized equation in [16, (4.3)] for τ values beyond the discontinuity). The mistake carries over to the formula [16, (4.24)] for $D_2X(a, \bar{S})\psi$, the formula [16, (4.25)] for $D_2\mathcal{F}(a, \bar{S})\psi$, as well as the linearized system [16, (4.31)–(4.32)] and makes them incorrect beyond the discontinuity for discontinuous g (the difference does not show for continuous g). We here present new versions of these formulas along with a new derivation of $D_3x(\tau; a, \bar{S})\psi$ based on differentiating the integrated ODE w.r.t. ψ. This new derivation provides a confirmation of the new formula. The authors of [16] are now aware of this and they informed us that a corrigendum is in preparation [15], consistent with our derivation of the linearization. Similarly, also the formula for $D_3x(\tau; a, \bar{S})\psi$ between [11, (A.9)] and [11, (A.10)] is incorrect. Below, with slight

abuse, we adopt the notation $\beta(a) := \beta(X(a,\bar S),\bar S)$, $\beta^+ := \lim_{a\downarrow \bar a_A}\beta(a)$, $\beta^- := \lim_{a\uparrow \bar a_A}\beta(a)$, $\beta_1(a) := \partial\beta(x,y)/\partial x|_{(X(a,\bar S),\bar S)}$, and $\beta_2(a) := \partial\beta(x,y)/\partial y|_{(X(a,\bar S),\bar S)}$. The same holds for γ, g, and μ. Moreover, again for brevity, we set

$$\mathcal{K}(\alpha_1,\alpha_2) := e^{\int_{\alpha_2}^{\alpha_1} g_1(\theta)d\theta} g_2(\alpha_2), \tag{1.6}$$

$$\mathcal{H}(\alpha_1,\alpha_2) := -\mathcal{F}(\alpha_1,\bar S)\left(\int_{\alpha_2}^{\alpha_1}\mu_1(\theta)\mathcal{K}(\theta,\alpha_2)d\theta + \mu_2(\alpha_2)\right). \tag{1.7}$$

We obtain

$$\begin{aligned} D_2X(a,\bar S)\psi = {} & \int_0^a \mathcal{K}(a,\alpha)\psi(-a+\alpha)d\alpha + H(a-\bar a_A)\left(\frac{g^+}{g^-}-1\right) \\ & \cdot\int_0^{\bar a_A}\mathcal{K}(a,\alpha)\psi(-a+\alpha)d\alpha, \end{aligned} \tag{1.8}$$

$$\begin{aligned} D_2\mathcal{F}(a,\bar S)\psi = {} & \int_0^a \mathcal{H}(a,\alpha)\psi(-a+\alpha)d\alpha + H(a-\bar a_A)\mathcal{F}(a,\bar S) \\ & \cdot\int_0^{\bar a_A}\left[\frac{\mu^- - \mu^+}{g^-}\mathcal{K}(\bar a_A,\alpha) - \left(\frac{g^+}{g^-}-1\right)\int_{\bar a_A}^a \mu_1(\sigma)\mathcal{K}(\sigma,\alpha)d\sigma\right]\psi(-a+\alpha)d\alpha, \end{aligned} \tag{1.9}$$

where H denotes the Heaviside function. We also get

$$Da_A(\bar S)\psi = -\frac{1}{g^-}\int_0^{\bar a_A}\mathcal{K}(\bar a_A,\alpha)\psi(-\bar a_A+\alpha)d\alpha, \tag{1.10}$$

which is consistent with [16, (4.30)]. We refer to Appendix A for a more detailed derivation. Now we have all the tools for the linearization of (1.4)–(1.5) with (1.2)–(1.3). Thus, for $y(t)$ and $z(t)$ small perturbations in the neighborhood of $\bar b$ and $\bar S$, respectively, the corrected linearized system reads

$$\begin{aligned} y(t) = {} & \int_{\bar a_A}^h \beta(a)\mathcal{F}(a,\bar S)y(t-a)da + \left(\bar b\int_{\bar a_A}^h \beta_2(a)\mathcal{F}(a,\bar S)da\right)z(t) \\ & + \frac{\bar b\beta^+}{g^-}\mathcal{F}(\bar a_A,\bar S)\int_0^{\bar a_A}\mathcal{K}(\bar a_A,\bar a_A-a)z(t-a)da \\ & + \bar b\int_0^h\left\{\int_{\max\{\bar a_A,a\}}^{\min\{a+\bar a_A,h\}}\mathcal{F}(\sigma,\bar S)\left[\frac{\mu^- - \mu^+}{g^-}\beta(\sigma)\mathcal{K}(\bar a_A,\sigma-a)\right.\right. \\ & \left. + \left(\frac{g^+}{g^-}-1\right)\left(\beta_1(\sigma)\mathcal{K}(\sigma,\sigma-a) - \beta(\sigma)\int_{\bar a_A}^\sigma \mu_1(\rho)\mathcal{K}(\rho,\sigma-a)d\rho\right)\right]d\sigma \\ & \left. + \int_{\max\{\bar a_A,a\}}^h\left[\beta_1(\sigma)\mathcal{F}(\sigma,\bar S)\mathcal{K}(\sigma,\sigma-a) + \beta(\sigma)\mathcal{H}(\sigma,\sigma-a)\right]d\sigma\right\}z(t-a)da, \end{aligned} \tag{1.11}$$

$$\begin{aligned} z'(t) = {} & \left(f'(\bar S) - \bar b\int_0^h \gamma_2(a)\mathcal{F}(a,\bar S)da\right)z(t) - \int_0^h \gamma(a)\mathcal{F}(a,\bar S)y(t-a)da \\ & - \frac{\bar b(\gamma^+ - \gamma^-)}{g^-}\mathcal{F}(\bar a_A,\bar S)\int_0^{\bar a_A}\mathcal{K}(\bar a_A,\bar a_A-a)z(t-a)da \end{aligned} \tag{1.12}$$

$$-\bar{b}\int_0^h \left\{ \int_{\max\{\bar{a}_A,a\}}^{\min\{a+\bar{a}_A,h\}} \mathcal{F}(\sigma,\bar{S})\left[\frac{\mu^- - \mu^+}{g^-}\gamma(\sigma)\mathcal{K}(\bar{a}_A,\sigma-a)\right.\right.$$
$$\left. + \left(\frac{g^+}{g^-}-1\right)\left(\gamma_1(\sigma)\mathcal{K}(\sigma,\sigma-a) - \gamma(\sigma)\int_{\bar{a}_A}^{\sigma}\mu_1(\rho)\mathcal{K}(\rho,\sigma-a)d\rho\right)\right] d\sigma$$
$$\left. + \int_a^h \left[\gamma_1(\sigma)\mathcal{F}(\sigma,\bar{S})\mathcal{K}(\sigma,\sigma-a) + \gamma(\sigma)\mathcal{H}(\sigma,\sigma-a)\right] d\sigma \right\} z(t-a)da.$$

A corresponding characteristic equation is obtained in [11, 16] by looking for nontrivial exponential solutions of (1.11)–(1.12). Then, the principle of linearized stability states that an equilibrium is locally asymptotically stable if all the characteristic roots have negative real part, whereas it is unstable if at least one characteristic root has positive real part. This principle is essential in [11] for computing stability boundaries in a chosen parameter plane using numerical continuation [1]. Indeed, a necessary condition to switch stability is that a characteristic root (or a pair of complex-conjugate roots) crosses the imaginary axis with positive speed. As a consequence, in [11] a point in the parameter plane is considered to belong to a stability boundary if an equilibrium exists and $i\omega$ solves the characteristic equation for some real ω. Then, continuation under parameter variation allows us to obtain transcritical bifurcation curves (switches from a stable trivial equilibrium to an unstable trivial and a stable positive equilibrium) and Hopf bifurcation curves (switches from a stable positive equilibrium to an unstable positive equilibrium and a stable periodic solution). Although rather useful, this technique based on the characteristic equation may present difficulties from both the theoretical and computational points of view: it is not trivial to obtain a solution point to start the continuation; it is not guaranteed that $i\omega$ is the rightmost (stability determining) root; it is not guaranteed that $i\omega$ crosses the imaginary axis with positive speed; inaccurate results may appear due to ill-conditioning (see, e.g., the discussion at the end of [7, section 1.1]). Overcoming these difficulties motivates the present work: in the next section we reformulate the problem from a dynamical systems point of view and follow the similar approach in [3].

1.3. Reformulation in infinite dimension. For $d_1, d_2 \in \mathbb{N}$ and $\tau > 0$, we introduce the Banach spaces of functions $Y := L_1([-\tau,0];\mathbb{R}^{d_1})$ and $Z := C([-\tau,0];\mathbb{R}^{d_2})$, equipped with the norms $\|\phi\|_Y = \int_{-\tau}^0 |\phi(\theta)|d\theta$ and $\|\psi\|_Z = \max_{\theta\in[-\tau,0]}|\psi(\theta)|$, respectively, $|\cdot|$ being any finite dimensional norm. The approach we intend to follow is suitable for the more general class of systems of linear VFEs/DDEs,

$$\begin{cases} y(t) = L_{11}y_t + L_{12}z_t, \\ z'(t) = L_{21}y_t + L_{22}z_t, \end{cases} \tag{1.13}$$

for $t \geq 0$, where $y_t \in Y$ and $z_t \in Z$ are the histories (or states) of the system at time t, recalling that they are respectively defined as $y_t(\theta) := y(t+\theta)$ and $z_t(\theta) := z(t+\theta)$ for $\theta \in [-\tau, 0]$ and $L_{11} : Y \to \mathbb{R}^{d_1}$, $L_{12} : Z \to \mathbb{R}^{d_1}$, $L_{21} : Y \to \mathbb{R}^{d_2}$, and $L_{22} : Z \to \mathbb{R}^{d_2}$ are given linear continuous functionals. In general, (1.13) comes from the linearization of

$$\begin{cases} b(t) = F_1(b_t, S_t), \\ S'(t) = F_2(b_t, S_t) \end{cases} \tag{1.14}$$

around an equilibrium $(\bar{b}, \bar{S})$, where $F_1 : Y \times Z \to \mathbb{R}^{d_1}$ and $F_2 : Y \times Z \to \mathbb{R}^{d_2}$ are sufficiently smooth nonlinear functionals. By using the norm $\|(\phi,\psi)\|_{Y\times Z} :=$

$\|\phi\|_Y + \|\psi\|_Z$, the infinite dimensional product space $Y \times Z$ is a Banach space. In what follows, an element $(\phi, \psi) \in Y \times Z$ denotes the function $(\phi, \psi) : [-\tau, 0] \to \mathbb{R}^{d_1+d_2}$ s.t. $(\phi, \psi)(\theta) = (\phi(\theta), \psi(\theta))$ for $\theta \in [-\tau, 0]$ is considered as the column vector of the d_1 components of $\phi(\theta)$ followed by the d_2 components of $\psi(\theta)$. We remark that here $\mathbb{R}^{d_1+d_2}$ identifies $\mathbb{R}^{d_1} \times \mathbb{R}^{d_2}$, so let us be licensed to denote the elements of the former as couples (r, s) for $r \in \mathbb{R}^{d_1}$ and $s \in \mathbb{R}^{d_2}$.

Note that (1.4)–(1.5) and (1.11)–(1.12) are particular instances of (1.14) and (1.13), respectively, with $d_1 = d_2 = 1$, $\tau = h$, and functionals most of which are of integral type due to the continuous age distribution. Moreover, such functionals are given implicitly in terms of solutions of external ODEs: (1.2)–(1.3) for the nonlinear problem and the corresponding linearized ones for (1.11)–(1.12), which account for (1.6)–(1.7).

With the aim at reformulating (1.13) on $Y \times Z$, we introduce the solution operator $T(t)$ as the linear bounded operator $T(t) : Y \times Z \to Y \times Z$ defined by $T(t)(\phi, \psi) = (y_t, z_t)$ for $t \geq 0$. The family $\{T(t)\}_{t\geq 0}$ is a C_0-semigroup with infinitesimal generator the linear unbounded operator $\mathcal{A} : D(\mathcal{A}) \subseteq Y \times Z \to Y \times Z$ given by

$$\mathcal{A}(\phi, \psi) = (\phi', \psi'), \tag{1.15}$$

$$D(\mathcal{A}) = \{(\phi, \psi) \in Y \times Z : \ (\phi', \psi') \in Y \times Z \text{ and } (\phi, \psi')(0) = L(\phi, \psi)\} \tag{1.16}$$

for $L : Y \times Z \to \mathbb{R}^{d_1+d_2}$ defined as

$$L(\phi, \psi) := (L_{11}\phi + L_{12}\psi, L_{21}\phi + L_{22}\psi). \tag{1.17}$$

It follows that the Cauchy problem for (1.13) with initial functions $y_0 = \phi$ and $z_0 = \psi$ for $(\phi, \psi) \in D(\mathcal{A})$ is equivalent to the abstract Cauchy problem

$$\begin{cases} \dfrac{d}{dt}(u(t), v(t)) = \mathcal{A}(u(t), v(t)), & t \geq 0, \\ (u(0), v(0)) = (\phi, \psi), \end{cases}$$

in the sense that $(y_t, z_t) = (u(t), v(t))$ for all $t \geq 0$. We refer to [20] for a general treatment of one-parameter semigroups, their generation and spectral theories, as well as their application to evolution equations. We instead refer to [14] for the specific case of VFEs/DDEs (see also [18] for DDEs), from which the (above and the) following fundamental results are obtained by using the sun-star theory of dual semigroups.

THEOREM 1.1. *The spectrum $\sigma(\mathcal{A})$ of $\mathcal{A}$ contains only eigenvalues of finite algebraic multiplicity and every right half-plane in $\mathbb{C}$ contains at most finitely many eigenvalues. Moreover, $\lambda \in \sigma(\mathcal{A})$ iff it is a root of the characteristic equation*

$$\det \begin{pmatrix} I_{d_1} - L_{11}e^{\lambda \cdot} I_{d_1} & -L_{12}e^{\lambda \cdot} I_{d_2} \\ -L_{21}e^{\lambda \cdot} I_{d_1} & \lambda I_{d_2} - L_{22}e^{\lambda \cdot} I_{d_2} \end{pmatrix} = 0,$$

and the algebraic multiplicity of λ coincides with its order as a characteristic root.

THEOREM 1.2 (principle of linearized stability). *An equilibrium of* (1.14) *is locally asymptotically stable if $\Re(\lambda) < 0$ for all $\lambda \in \sigma(\mathcal{A})$, whereas it is unstable if $\Re(\lambda) > 0$ for at least one $\lambda \in \sigma(\mathcal{A})$.*

By virtue of the above reformulation we first transform the problem of computing the characteristic roots into that of computing the eigenvalues of $\mathcal{A}$. Consequently, the problem of determining the stability of an equilibrium is translated into the problem of computing the rightmost eigenvalue(s) of $\mathcal{A}$. Now, by following the numerical

approach in [3], we approximate (a finite number of) the eigenvalues of $\mathcal{A}$ by the eigenvalues of a finite dimensional linear operator that discretizes $\mathcal{A}$, i.e., a matrix $\mathcal{A}_M$. This approximation is a natural extension of the pseudospectral method developed in [4] for DDEs and in [5] also for VFEs, then resulted in the method for systems of VFEs/DDEs investigated in [3]. For DDEs see also the more recent exposition [7].

The new contributions of the present work w.r.t. [3] follow: (i) we modify the treatment of the nonlocal boundary condition in $D(\mathcal{A})$ to allow for a future extension in view of the approach proposed in [27], directly applicable to nonlinear problems (1.14) without the unavoidable difficulties posed by the method in [3] consisting in reformulating the problem and using additional numerical root finders; (ii) for the first time we rigorously prove the spectral accuracy (see, e.g., [32]) of the approximated eigenvalues and furnish an upper bound for the error; (iii) we extend the approach to realistic Daphnia models (1.4)–(1.5) by including the numerical solution of the external ODEs (1.2)–(1.3), the quadrature of the integrals at the right-hand sides of (1.4)–(1.5) whose integrands are given implicitly through the solutions of the above ODEs, and the treatment of the juveniles-adults discontinuities; (iv) we discuss a detailed implementation to suitably tackle all the above points and consequently study the influence of the various error sources on the main spectral convergence rate; (v) we test the method on a realistic Daphnia model and compare with data from [11], recalling also that both the model and the data are based on experimental evidence.

2. Numerical method and convergence analysis. Given a positive integer M, let $\Omega_M = \{\theta_0, \theta_1, \dots, \theta_M\}$ be a mesh of points on $[-\tau, 0]$ satisfying $-\tau =: \theta_M < \cdots \theta_1 < \theta_0 := 0$. We replace the infinite dimensional state space $Y \times Z$ by the finite dimensional state space $Y_M \times Z_M$ of the discrete functions defined on Ω_M by choosing $Y_M := (\mathbb{R}^{d_1})^{\Omega_M \setminus \{0\}} \cong \mathbb{R}^{d_1 M}$ and $Z_M := (\mathbb{R}^{d_2})^{\Omega_M} \cong \mathbb{R}^{d_2(M+1)}$. An element $(\Phi, \Psi) \in Y_M \times Z_M$ is intended as the column vector formed by the M components of $\Phi = (\Phi_1, \dots, \Phi_M) \in Y_M$ followed by the $M+1$ components of $\Psi = (\Psi_0, \Psi_1, \dots, \Psi_M) \in Z_M$, where $\Phi_i \in \mathbb{R}^{d_1}$ for $i = 1, \dots, M$ and $\Psi_i \in \mathbb{R}^{d_2}$ for $i = 0, 1, \dots, M$.

We remark that it is not always possible to compute the exact functionals L_{11}, L_{12}, L_{21}, and L_{22} in (1.13). This is the case of (1.11)–(1.12) for, e.g., the integral form of the functionals. Let then $\tilde{L}_{11}$, $\tilde{L}_{12}$, $\tilde{L}_{21}$, and $\tilde{L}_{22}$ be suitable computable approximations and define $\tilde{L}$ analogously to L in (1.17). These approximations are the argument of section 3.

Given $(\Phi, \Psi) \in Y_M \times Z_M$, consider $(P_M, Q_M) \in Y \times Z$, where P_M and Q_M are the polynomials of degree at most M uniquely determined by

$$P_M(\theta_0) = \tilde{L}_{11} P_M + \tilde{L}_{12} Q_M, \tag{2.1}$$

$$P_M(\theta_i) = \Phi_i, \qquad i = 1, \dots, M, \tag{2.2}$$

$$Q_M(\theta_i) = \Psi_i, \qquad i = 0, 1, \dots, M. \tag{2.3}$$

Through such polynomials we construct a finite dimensional linear operator $\mathcal{A}_M : Y_M \times Z_M \to Y_M \times Z_M$ as

$$\mathcal{A}_M(\Phi, \Psi) = (\xi, \eta), \tag{2.4}$$

where

$$\xi_i = P'_M(\theta_i), \qquad i = 1, \dots, M, \tag{2.5}$$

$$\eta_0 = \tilde{L}_{21} P_M + \tilde{L}_{22} Q_M, \tag{2.6}$$

$$\eta_i = Q'_M(\theta_i), \qquad i = 1, \dots, M. \tag{2.7}$$

The linearity of $\mathcal{A}_M$ follows from the linearity of interpolation, differentiation, (2.1), and (2.6). The action (2.4) of $\mathcal{A}_M$ mimics the action (1.15) of $\mathcal{A}$ through (2.5) and (2.7). Moreover, the nonlocal boundary condition in the domain (1.16) of $\mathcal{A}$ is discretized through (2.1) and (2.6). In section 3.2, with abuse of notation, we denote by $\mathcal{A}_M$ also the matrix in $\mathbb{R}^{(d_1M+d_2(M+1))\times(d_1M+d_2(M+1))}$ representing (2.4) in the canonical basis. There we construct explicit entries for the Daphnia case (1.11)–(1.12).

We underline that the above treatment of the boundary condition through (2.1) and (2.6) is different from that in [3], where basically (2.6) is removed from (2.4) and replaced by $Q_M(\theta_0) = \tilde{L}_{21}P_M + \tilde{L}_{22}Q_M$. The latter is solved explicitly in the construction of Q_M, as it occurs for P_M in (2.1). The choice is motivated as follows. In [27] a generalization of this pseudospectral discretization is applied directly to systems of nonlinear VFEs/DDEs like (1.14). It is the intention of (some of) the authors together with the author of [27] to apply this extension to Daphnia models. For the latter class with reference to (1.14), only F_1 is linear w.r.t. b, while F_2 is in general nonlinear w.r.t. S. This makes (2.1) explicitly solvable for $P_M(\theta_0)$, whereas the analogue for $Q_M(\theta_0)$ is no longer true. Hence the method proposed in [3] would require an additional numerical solver for nonlinear equations, opposite to the method proposed here. As a further reasoning, this version is the logic coupling of the method in [4] for DDEs with the method in [5] for VFEs, whereas the version in [3] requires an ulterior reformulation of the problem. Finally, the proof of convergence we give in section 2.1 can be adapted straightforwardly to [3], where a rigorous proof is lacking.

From now on we use the term *continuous* for the exact problem in infinite dimension, i.e., the computation of $\sigma(\mathcal{A})$, and the term *discrete* for the approximated problem in finite dimension, i.e., the computation of $\sigma(\mathcal{A}_M)$.

2.1. Error bounds and convergence. The convergence analysis of the discrete eigenvalues to the continuous ones combines the same arguments adopted in [4] for DDEs and in [5] for VFEs. The necessary steps follow: (i) recover the continuous and discrete characteristic equations by considering a suitable ODE Cauchy problem and its polynomial collocation; (ii) find a bound for the collocation error; (iii) bound the error between the characteristic equations in terms of the latter; and (iv) bound the error between the eigenvalues by applying Rouché's theorem (see, e.g., [9]). Here we revisit completely steps (i) and (ii): the former because the discretization is different from [3], the latter because in [5] the state space Y for the VFE part is assumed to be C instead of L_1 as it is assumed more properly in this work and according to [14]. This requires interpolation results sharper than those used in [4, 5]. Moreover, we work on the product state space $Y \times Z$ rather than on a single space. As far as steps (iii) and (iv) are concerned, we state only the final convergence result since the proof can be adapted straightforwardly from, e.g., [4, 7]. Notice that since the following analysis concerns eigenvalues, we implicitly merge the problem in $\mathbb{C}$, i.e., we assume $Y := L_1([-\tau, 0]; \mathbb{C}^{d_1})$ and $Z := C([-\tau, 0]; \mathbb{C}^{d_2})$.

We start with step (i). Let $\lambda \in \mathbb{C}$ and $(\phi, \psi) \in D(\mathcal{A}) \setminus \{(0, 0)\}$ be s.t. $\mathcal{A}(\phi, \psi) = \lambda(\phi, \psi)$, i.e.,

$$\begin{cases} (\phi', \psi')(\theta) = \lambda(\phi, \psi)(\theta), & \theta \in [-\tau, 0], \\ (\phi, \psi')(0) = L(\phi, \psi), \end{cases}$$

by virtue of (1.15) and (1.16). Since the solution of the ODE Cauchy problem

$$\begin{cases} (\phi', \psi')(\theta) = \lambda(\phi, \psi)(\theta), & \theta \in [-\tau, 0], \\ (\phi, \psi)(0) = (u_0, v_0), \end{cases} \tag{2.8}$$

is $(\phi,\psi) = e^{\lambda\cdot}(u_0,v_0) \in Y \times Z$ for $(u_0,v_0) \in \mathbb{C}^{d_1+d_2}$, we conclude that $\lambda \in \sigma(\mathcal{A})$ iff there exists $(u_0,v_0) \in \mathbb{C}^{d_1+d_2} \setminus \{(0,0)\}$ s.t. $(u_0,\lambda v_0) = Le^{\lambda\cdot}(u_0,v_0)$. Accordingly, we define the linear operator $\hat{\mathcal{A}}(\lambda) : \mathbb{C}^{d_1+d_2} \to \mathbb{C}^{d_1+d_2}$ as $\hat{\mathcal{A}}(\lambda)(u_0,v_0) := Le^{\lambda\cdot}(u_0,v_0)$ and the relevant characteristic function

$$c(\lambda) := \det\left(\begin{pmatrix} I_{d_1} & 0 \\ 0 & \lambda I_{d_2}\end{pmatrix} - \hat{\mathcal{A}}(\lambda)\right).$$

Then, $\lambda \in \sigma(\mathcal{A})$ iff the continuous characteristic equation $c(\lambda) = 0$ holds.

We proceed similarly for the discrete problem. Let $\lambda \in \mathbb{C}$ and $(\Phi,\Psi) \in Y_M \times Z_M \setminus \{(0,0)\}$ be s.t. $\mathcal{A}_M(\Phi,\Psi) = \lambda(\Phi,\Psi)$, i.e.,

$$\begin{cases} (P_M', Q_M')(\theta_i) = \lambda(P_M,Q_M)(\theta_i), & i = 1,\dots,M, \\ (P_M,Q_M')(\theta_0) = \tilde{L}(P_M,Q_M), \end{cases}$$

by virtue of (2.1)–(2.3), (2.4), and (2.5)–(2.7). By using the shorthand notation $p_M(\cdot) := p_M(\cdot;\lambda,(u_0,v_0))$ and $q_M(\cdot) := q_M(\cdot;\lambda,(u_0,v_0))$, we denote with $(p_M,q_M) \in Y \times Z$ the collocation polynomial of (2.8) on Ω_M, i.e.,

$$\begin{cases} (p_M', q_M')(\theta_i) = \lambda(p_M,q_M)(\theta_i), & i = 1,\dots,M, \\ (p_M,q_M)(\theta_0) = (u_0,v_0). \end{cases} \tag{2.9}$$

We conclude that $\lambda \in \sigma(\mathcal{A}_M)$ iff $(p_M,q_M) = (P_M,Q_M)$, that is, iff $(u_0,\lambda v_0) = \tilde{L}(p_M,q_M)$. Accordingly, we define the linear operator $\hat{\mathcal{A}}_M(\lambda) : \mathbb{C}^{d_1+d_2} \to \mathbb{C}^{d_1+d_2}$ as $\hat{\mathcal{A}}_M(\lambda)(u_0,v_0) := \tilde{L}(p_M,q_M)$ and the relevant characteristic function

$$c_M(\lambda) := \det\left(\begin{pmatrix} I_{d_1} & 0 \\ 0 & \lambda I_{d_2}\end{pmatrix} - \hat{\mathcal{A}}_M(\lambda)\right).$$

Then, $\lambda \in \sigma(\mathcal{A}_M)$ iff the discrete characteristic equation $c_M(\lambda) = 0$ holds.

Now we proceed with step (ii) and give an upper bound for the error of the collocation polynomial (p_M,q_M) in (2.9) as an approximation of the exponential solution $e^{\lambda\cdot}(u_0,v_0)$ of (2.8). To increase readability, we first collect a couple of preliminary results on the integral Volterra operator $K_\lambda : Y \times Z \to Y \times Z$ defined as

$$(K_\lambda(\phi,\psi))(\theta) := \lambda \int_0^\theta (\phi,\psi)(s)ds, \qquad \theta \in [-\tau,0],$$

for $\lambda \in \mathbb{C}$ and on the Lagrange interpolation operator $\mathcal{L}_{M-1} : Y \times Z \to Y \times Z$ relevant to the nodes $\theta_1,\dots,\theta_M$ in Ω_M. Both these operators are linear and bounded. In what follows we set $I := I_{Y\times Z}$ and $\|\cdot\| := \|\cdot\|_{Y\times Z \leftarrow Y\times Z}$ for the operator-induced norm.

LEMMA 2.1. *$I - K_\lambda$ is invertible and $\|(I-K_\lambda)^{-1}\| \le e^{|\lambda|\tau}$.*

Proof. Invertibility follows from standard theory on linear integral equations (see, e.g., [24]). For $(y,z) \in Y \times Z$ consider $(\xi,\eta) \in Y \times Z$ as the unique solution of $(I-K_\lambda)(\xi,\eta) = (y,z)$, i.e., componentwise for $\theta \in [-\tau,0]$, $\xi(\theta) = y(\theta) + \lambda\int_0^\theta \xi(s)ds$ and $\eta(\theta) = z(\theta) + \lambda\int_0^\theta \eta(s)ds$. Then, for all $\sigma \in [-\tau,0]$,

$$\int_\sigma^0 |\xi(\theta)|d\theta = \int_\sigma^0 \left| y(\theta) + \lambda\int_0^\theta \xi(s)ds \right| d\theta \le \int_\sigma^0 |y(\theta)|d\theta + |\lambda| \int_\sigma^0 \left(\int_\theta^0 |\xi(s)|ds \right) d\theta,$$

$$\max_{\theta\in[\sigma,0]} |\eta(\theta)| = \max_{\theta\in[\sigma,0]} \left| z(\theta) + \lambda\int_0^\theta \eta(s)ds \right| \le \max_{\theta\in[\sigma,0]} |z(\theta)| + |\lambda| \int_\sigma^0 \max_{\theta\in[s,0]} |\eta(\theta)|ds.$$

The bound on $\|(I-K_\lambda)^{-1}\|$ follows by applying Gronwall's lemma to both the latter and by considering $\sigma=-\tau$, since we get $\|(\xi,\eta)\|_{Y\times Z}\le e^{|\lambda|\tau}\|(y,z)\|_{Y\times Z}$. ∎

Assumption 2.2. *Let Ω_M be made of Chebyshev extremal nodes:*

$$\theta_i=\frac{\tau}{2}\left(\cos\left(\frac{i\pi}{M}\right)-1\right),\qquad i=0,1,\dots,M.$$

LEMMA 2.3. *Under Assumption* 2.2, $\|(\mathcal{L}_{M-1}-I)K_\lambda\|\to 0$ *as* $M\to\infty$.

Proof. $K_\lambda(Y\times Z)$ is a subset of the space of absolutely continuous functions $[-\tau,0]\to\mathbb{C}^{d_1+d_2}$. The thesis follows from the sharp interpolation results in [25]. ∎

Now we denote by $B(\lambda,\rho)$ the closed ball in $\mathbb{C}$ of center λ and radius ρ and give the collocation result.

THEOREM 2.4. *Let $\lambda^*\in\mathbb{C}$ and $\rho_0>0$. Under Assumption* 2.2*, there exists $M_0\in\mathbb{N}$ s.t. for all $M\ge M_0$, all $\lambda\in B(\lambda^*,\rho_0)$, and all $(u_0,v_0)\in\mathbb{C}^{d_1+d_2}$, the collocation polynomial of* (2.8) *given by* (2.9) *exists, is unique, and satisfies*

$$\|(p_M(\cdot;\lambda,(u_0,v_0)),q_M(\cdot;\lambda,(u_0,v_0)))-e^{\lambda\cdot}(u_0,v_0)\|_{Y\times Z}\le\frac{C_0}{\sqrt{M}}\left(\frac{C_1}{M}\right)^M|(u_0,v_0)|$$

with C_0 and C_1 constants independent of M.

Proof. We rewrite (2.8) and (2.9) as the functional equations in $Y\times Z$

$$(\phi,\psi)=(u_0,v_0)+K_\lambda(\phi,\psi),\qquad (p_M,q_M)=(u_0,v_0)+K_\lambda\mathcal{L}_{M-1}(p_M,q_M),$$

where, with abuse of notation, $(u_0,v_0)\in Y\times Z$ is the function of constant value $(u_0,v_0)\in\mathbb{C}^{d_1+d_2}$. By subtracting we get

$$e_M=K_\lambda\mathcal{L}_{M-1}e_M+K_\lambda r_M \tag{2.10}$$

for the collocation error $e_M:=(p_M,q_M)-(\phi,\psi)$, where $r_M:=(\mathcal{L}_{M-1}-I)(\phi,\psi)$ is the interpolation remainder on the exponential solution of (2.8). The solutions of (2.10) are the functions $e_M=K_\lambda\hat{e}_M$ for $\hat{e}_M$ a solution of

$$\hat{e}_M=\mathcal{L}_{M-1}K_\lambda\hat{e}_M+r_M. \tag{2.11}$$

By virtue of Lemmas 2.1 and 2.3 we can apply a corollary of the Banach perturbation lemma (see, e.g., [24, Theorem 10.1]) to get that there exists $M_0\in\mathbb{N}$ s.t. for all $M\ge M_0$ and independently of λ the operator $I-\mathcal{L}_{M-1}K_\lambda$ is invertible and $\|(I-\mathcal{L}_{M-1}K_\lambda)^{-1}\|\le 2\|(I-K_\lambda)^{-1}\|$. This implies in cascade that (2.11), (2.10), and (2.9) admit a unique solution. Moreover,

$$\|e_M\|_{Y\times Z}\le 2\|K_\lambda\|\|(I-K_\lambda)^{-1}\|\|r_M\|_{Y\times Z}.$$

Beyond numerical constants, for the first factor at the right-hand side it is not difficult to prove that $\|K_\lambda\|\le|\lambda|\tau$ by recalling that $\|(y,z)\|_{Y\times Z}=\|y\|_Y+\|z\|_Z$. For the second factor Lemma 2.1 holds. For the third factor we obtain

$$\|r_M\|_{Y\times Z}\le\frac{(|\lambda|\tau)^M}{M!}\max\{1,e^{-\Re(\lambda)\tau}\}|(u_0,v_0)|$$

by applying the standard Cauchy's remainder for interpolation, since the interpolated function is the exponential solution of (2.8). The final bound on the collocation error is a direct consequence of Stirling's approximation $M!\ge\sqrt{2\pi M}(M/e)^M$. ∎

Now, as anticipated, we conclude the convergence analysis by stating without proof a theorem on the error between continuous and discrete eigenvalues. This final result accounts for steps (iii) and (iv) and can be recovered by following [4, Lemmas 3.4 and 3.5, Theorem 3.6] in a straightforward manner.

Assumption 2.5. *$\tilde{L}$ is bounded.*

THEOREM 2.6. *Let $\lambda^* \in \sigma(\mathcal{A})$ with multiplicity ν. Under Assumptions* 2.2 *and* 2.5*, there exist $\rho_0 > 0$ and $M_0 \in \mathbb{N}$ s.t. for all $M \geq M_0$ and for sufficiently small*

$$\varepsilon := \sup_{\substack{\lambda \in B(\lambda^*, \rho_0) \\ (u_0, v_0) \in \mathbb{C}^{d_1+d_2} \setminus \{(0,0)\}}} \frac{|Le^{\lambda \cdot}(u_0, v_0) - \tilde{L}e^{\lambda \cdot}(u_0, v_0)|}{|(u_0, v_0)|},$$

there exist $\lambda_i \in \sigma(\mathcal{A}_M)$, $i = 1, \ldots, \nu$, counted with multiplicities, satisfying

$$\max_{i=1,\ldots,\nu} |\lambda^* - \lambda_i| \leq C_2 \left(\varepsilon + \frac{1}{\sqrt{M}} \left(\frac{C_1}{M} \right)^M \right)^{\frac{1}{\nu}} \tag{2.12}$$

with C_1 and C_2 constants independent of M.

The term ε in (2.12) takes into account the approximation $\tilde{L}$ of the exact right-hand side L of (1.13). As already remarked, for realistic Daphnia models such as (1.11)–(1.12), this quantity accounts for the error committed in the numerical solution of the external ODEs (1.2)–(1.3), as well as in the numerical quadrature of the integrals at the right-hand side of (1.11)–(1.12). These contributions are discussed in section 3. However, in general, one can guarantee that $\varepsilon < \text{TOL}$ for a given tolerance TOL (e.g., machine precision). If so, the meaning of (2.12) is that, modulo multiplicity, the error falls down to TOL by following a spectrally accurate behavior, i.e., $O(M^{-M})$. Finally, we also remark that by virtue of [4, Proposition 3.7], the existence of physically spurious eigenvalues [2, Chapter 7] is excluded: all the eigenvalues of $\mathcal{A}_M$ converge to eigenvalues of $\mathcal{A}$ as $M \to \infty$.

Finally, we wish to remark that, beyond the above analysis of the analytic errors, other numerical and computational issues should be taken into account in general when approximating infinite dimensional eigenvalue problems through collocation, for instance, the role of the constant C_1 in (2.12), whose value can be easily recovered from the proof of Theorem 2.4 and guarantees higher accuracy for eigenvalues of smaller magnitudes. This and other general aspects of the method have been appropriately commented on in [3, 4, 6, 7]. As a general and cornerstone reference see [2, Chapter 7], where a heuristic rule of thumb for the choice of M is established and spurious solutions are adequately treated, and also the recent monograph [21] for challenging nonstandard eigenvalue problems, where suitable eigenvalue solvers in finite dimension are also discussed, like, e.g., Jacobi–Davidson type methods [28].

3. Numerical implementation. In this section we construct the matrix $\mathcal{A}_M$ relevant to the linear operator (2.4) for realistic Daphnia models (1.11)–(1.12). Recall that $d_1 = d_2 = 1$. The exact linear functionals at the right-hand side of (1.13) are

$$L_{11}\phi = \int_{-h}^{-\bar{a}_A} B_{11}^{(A)}(\theta)\phi(\theta)d\theta, \tag{3.1}$$

$$L_{12}\psi = A_{12}\psi(0) + \int_{-\bar{a}_A}^{0} B_{12}^{(J)}(\theta)\psi(\theta)d\theta + \int_{-h}^{-\bar{a}_A} B_{12}^{(A)}(\theta)\psi(\theta)d\theta, \tag{3.2}$$

$$L_{21}\phi = \int_{-\bar{a}_A}^{0} B_{21}^{(J)}(\theta)\phi(\theta)d\theta + \int_{-h}^{-\bar{a}_A} B_{21}^{(A)}(\theta)\phi(\theta)d\theta, \tag{3.3}$$

$$L_{22}\psi = A_{22}\psi(0) + \int_{-\bar{a}_A}^{0} B_{22}^{(J)}(\theta)\psi(\theta)d\theta + \int_{-h}^{-\bar{a}_A} B_{22}^{(A)}(\theta)\psi(\theta)d\theta \tag{3.4}$$

for the scalars

$$A_{12} = \bar{b}\int_{\bar{a}_A}^{h} \beta_2(a)\mathcal{F}(a,\bar{S})da, \qquad A_{22} = f'(\bar{S}) - \bar{b}\int_{0}^{h} \gamma_2(a)\mathcal{F}(a,\bar{S})da$$

and the functions $B_{ij}^{(J)} : [-\bar{a}_A, 0] \to \mathbb{R}$ and $B_{ij}^{(A)} : [-h, -\bar{a}_A] \to \mathbb{R}$, $i,j = 1,2$ (excluding $B_{11}^{(J)}$), respectively given for the juveniles (superscript J) by

$$\begin{aligned}
B_{12}^{(J)}(\theta) &= \frac{\bar{b}\beta^+}{g^-}\mathcal{F}(\bar{a}_A,\bar{S})\mathcal{K}(\bar{a}_A,\bar{a}_A+\theta) \\
&\quad + \bar{b}\int_{\bar{a}_A}^{\min\{-\theta+\bar{a}_A,h\}} \mathcal{F}(\sigma,\bar{S})\Bigg[\frac{\mu^- - \mu^+}{g^-}\beta(\sigma)\mathcal{K}(\bar{a}_A,\sigma+\theta) \\
&\quad + \left(\frac{g^+}{g^-} - 1\right)\left(\beta_1(\sigma)\mathcal{K}(\sigma,\sigma+\theta) - \beta(\sigma)\int_{\bar{a}_A}^{\sigma}\mu_1(\rho)\mathcal{K}(\rho,\sigma+\theta)d\rho\right)\Bigg]d\sigma \\
&\quad + \bar{b}\int_{\bar{a}_A}^{h}\left[\beta_1(\sigma)\mathcal{F}(\sigma,\bar{S})\mathcal{K}(\sigma,\sigma+\theta) + \beta(\sigma)\mathcal{H}(\sigma,\sigma+\theta)\right]d\sigma, \\
B_{21}^{(J)}(\theta) &= -\gamma(-\theta)\mathcal{F}(-\theta,\bar{S}),
\end{aligned}$$

$$\begin{aligned}
B_{22}^{(J)}(\theta) &= -\frac{\bar{b}(\gamma^+ - \gamma^-)}{g^-}\mathcal{F}(\bar{a}_A,\bar{S})\mathcal{K}(\bar{a}_A,\bar{a}_A+\theta) \\
&\quad - \bar{b}\int_{\bar{a}_A}^{\min\{-\theta+\bar{a}_A,h\}} \mathcal{F}(\sigma,\bar{S})\Bigg[\frac{\mu^- - \mu^+}{g^-}\gamma(\sigma)\mathcal{K}(\bar{a}_A,\sigma+\theta) \\
&\quad + \left(\frac{g^+}{g^-} - 1\right)\left(\gamma_1(\sigma)\mathcal{K}(\sigma,\sigma+\theta) - \gamma(\sigma)\int_{\bar{a}_A}^{\sigma}\mu_1(\rho)\mathcal{K}(\rho,\sigma+\theta)d\rho\right)\Bigg]d\sigma \\
&\quad - \bar{b}\int_{-\theta}^{h}\left[\gamma_1(\sigma)\mathcal{F}(\sigma,\bar{S})\mathcal{K}(\sigma,\sigma+\theta) + \gamma(\sigma)\mathcal{H}(\sigma,\sigma+\theta)\right]d\sigma
\end{aligned}$$

and for the adults (superscript A) by

$$\begin{aligned}
B_{11}^{(A)}(\theta) &= \beta(-\theta)\mathcal{F}(-\theta,\bar{S}), \\
B_{12}^{(A)}(\theta) &= +\bar{b}\int_{-\theta}^{\min\{-\theta+\bar{a}_A,h\}} \mathcal{F}(\sigma,\bar{S})\Bigg[\frac{(\mu^- - \mu^+)}{g^-}\beta(\sigma)\mathcal{K}(\bar{a}_A,\sigma+\theta) \\
&\quad + \left(\frac{g^+}{g^-} - 1\right)\left(\beta_1(\sigma)\mathcal{K}(\sigma,\sigma+\theta) - \beta(\sigma)\int_{\bar{a}_A}^{\sigma}\mu_1(\rho)\mathcal{K}(\rho,\sigma+\theta)d\rho\right)\Bigg]d\sigma \\
&\quad + \bar{b}\int_{-\theta}^{h}\left[\beta_1(\sigma)\mathcal{F}(\sigma,\bar{S})\mathcal{K}(\sigma,\sigma+\theta) + \beta(\sigma)\mathcal{H}(\sigma,\sigma+\theta)\right]d\sigma, \\
B_{21}^{(A)}(\theta) &= -\gamma(-\theta)\mathcal{F}(-\theta,\bar{S}), \\
B_{22}^{(A)}(\theta) &= -\bar{b}\int_{-\theta}^{\min\{-\theta+\bar{a}_A,h\}} \mathcal{F}(\sigma,\bar{S})\Bigg[\frac{(\mu^- - \mu^+)}{g^-}\gamma(\sigma)\mathcal{K}(\bar{a}_A,\sigma+\theta)
\end{aligned}$$

$$+\left(\frac{g^+}{g^-}-1\right)\left(\gamma_1(\sigma)\mathcal{K}(\sigma,\sigma+\theta)-\gamma(\sigma)\int_{\bar a_A}^{\sigma}\mu_1(\rho)\mathcal{K}(\rho,\sigma+\theta)d\rho\right)\Bigg]d\sigma$$
$$-\bar b\int_{-\theta}^{h}\left[\gamma_1(\sigma)\mathcal{F}(\sigma,\bar S)\mathcal{K}(\sigma,\sigma+\theta)+\gamma(\sigma)\mathcal{H}(\sigma,\sigma+\theta)\right]d\sigma.$$

As anticipated in section 2, the functionals (3.1)–(3.4) cannot be evaluated exactly for a general choice of model rates. Therefore, approximation is needed for (i) computing the integrals in (3.1)–(3.4)—we call them the *outer* integrals; and (ii) evaluating the scalars A's and the functions B's, first, because $X(\cdot,\bar S)$ and $\mathcal{F}(\cdot,\bar S)$ are obtained as solutions of (1.2)–(1.3) which, in general, cannot be solved analytically, and second, for the presence of further integrals, which we call the *inner* integrals. In the following sections we address separately all these computational issues, eventually leading to the explicit construction of $\mathcal{A}_M$ through a piecewise variant of the method illustrated in section 2.

3.1. Quadrature of outer integrals. The integration intervals in (3.1)–(3.4) are separated between the juvenile and adult periods because of the possible discontinuities in the vital rates. It is then natural to separate the quadrature as well. On each interval, as suggested in [3], we adopt the interpolatory formula based on Chebyshev extremal nodes, known as the Clenshaw–Curtis formula [32, 33]. In general, for a positive integer n and $f:[a,b]\to\mathbb{R}$,

$$\int_a^b f(\theta)d\theta\approx\sum_{k=0}^{n}w_k f(\theta_k) \tag{3.5}$$

with w_k's and θ_k's the Clenshaw–Curtis weights and Chebyshev extremal nodes on $[a,b]$, respectively. Both are obtained straightforwardly from the weights and nodes on $[-1,1]$ by shift and scaling and can be computed efficiently as explained in [32].

To approximate the outer integrals by (3.5), let M_J and M_A be positive integers, possibly different. Define $M:=M_J+M_A$ and introduce on $[-h,0]$ the piecewise mesh $\Omega_M:=\Omega^{(J)}_{M_J}\bigcup\Omega^{(A)}_{M_A}$ with, respectively,

$$\Omega^{(J)}_{M_J}:=\left\{\theta_i^{(J)},\ i=0,1,\dots,M_J\ :\ \theta_i^{(J)}=\frac{\bar a_A}{2}\cos\left(\frac{i\pi}{M_J}\right)-\frac{\bar a_A}{2}\right\}, \tag{3.6}$$
$$\Omega^{(A)}_{M_A}:=\left\{\theta_i^{(A)},\ i=0,1,\dots,M_A\ :\ \theta_i^{(A)}=\frac{h-\bar a_A}{2}\cos\left(\frac{i\pi}{M_A}\right)-\frac{h+\bar a_A}{2}\right\} \tag{3.7}$$

the meshes of Chebyshev extremal nodes on $[-\bar a_A,0]$ and $[-h,-\bar a_A]$. Notice the superposition $\theta_0^{(A)}=-\bar a_A=\theta_{M_J}^{(J)}$. Then we define the approximated functionals as

$$\tilde L_{11}\phi:=\sum_{k=0}^{M_A}w_k^{(A)}\tilde B_{11}^{(A)}(\theta_k^{(A)})\phi(\theta_k^{(A)}), \tag{3.8}$$

$$\tilde{L}_{12}\psi := \tilde{A}_{12}\psi(0) + \sum_{k=0}^{M_J} w_k^{(J)} \tilde{B}_{12}^{(J)}(\theta_k^{(J)})\psi(\theta_k^{(J)}) + \sum_{k=0}^{M_A} w_k^{(A)} \tilde{B}_{12}^{(A)}(\theta_k^{(A)})\psi(\theta_k^{(A)}),$$

$$\tilde{L}_{21}\phi := \sum_{k=0}^{M_J} w_k^{(J)} \tilde{B}_{21}^{(J)}(\theta_k^{(J)})\phi(\theta_k^{(J)}) + \sum_{k=0}^{M_A} w_k^{(A)} \tilde{B}_{21}^{(A)}(\theta_k^{(A)})\phi(\theta_k^{(A)}),$$

$$\tilde{L}_{22}\psi := \tilde{A}_{22}\psi(0) + \sum_{k=0}^{M_J} w_k^{(J)} \tilde{B}_{22}^{(J)}(\theta_k^{(J)})\psi(\theta_k^{(J)}) + \sum_{k=0}^{M_A} w_k^{(A)} \tilde{B}_{22}^{(A)}(\theta_k^{(A)})\psi(\theta_k^{(A)}). \tag{3.9}$$

Here we use $\tilde{A}$'s and $\tilde{B}$'s instead of A's and B's to include the numerical solutions of the ODEs (see section 3.3) and the approximation of the inner integrals (see section 3.4).

The choice of a piecewise quadrature based on Chebyshev extremal nodes motivates the piecewise discretization illustrated next. Together they lead to a considerable cost reduction. Moreover, by assuming sufficiently smooth piecewise vital rates, as anticipated in section 1.1, the quadrature error is spectrally accurate [32, 33]. Consequently, its contribution to the term ε in the final error bound in Theorem 2.6 is of the same type of the error on the eigenvalues, i.e., $O(M^{-M})$.

3.2. Piecewise discretization. Correspondingly to (3.6)–(3.7), consider an element $(\Phi, \Psi) \in Y_M \times Z_M$ with components indexed as

$$\Phi = \left(\Phi_1^{(J)}, \dots, \Phi_{M_J}^{(J)}, \Phi_1^{(A)}, \dots, \Phi_{M_A}^{(A)}\right), \quad \Psi = \left(\Psi_0^{(J)}, \Psi_1^{(J)}, \dots, \Psi_{M_J}^{(J)}, \Psi_1^{(A)}, \dots, \Psi_{M_A}^{(A)}\right)$$

and construct a piecewise continuous polynomial $(P_M, Q_M) \in Y \times Z$ as follows. (P_M, Q_M) is a polynomial $(P_{M_J}^{(J)}, Q_{M_J}^{(J)})$ of degree at most M_J defined on $[-\bar{a}_A, 0]$ and a polynomial $(P_{M_A}^{(A)}, Q_{M_A}^{(A)})$ of degree at most M_A defined on $[-h, -\bar{a}_A]$. By using the Lagrange bases $\{\ell_0^{(J)}, \ell_1^{(J)}, \dots, \ell_{M_J}^{(J)}\}$ and $\{\ell_0^{(A)}, \ell_1^{(A)}, \dots, \ell_{M_A}^{(A)}\}$ relevant to (3.6) and (3.7), respectively, by following (2.2)–(2.3) we have

$$\begin{aligned}
P_{M_J}^{(J)}(\theta) &= \ell_0^{(J)}(\theta) P_{M_J}^{(J)}(\theta_0^{(J)}) + \sum_{j=1}^{M_J} \ell_j^{(J)}(\theta)\Phi_j^{(J)}, && \theta \in [-\bar{a}_A, 0],\\
P_{M_A}^{(A)}(\theta) &= \ell_0^{(A)}(\theta)\Phi_{M_J}^{(J)} + \sum_{j=1}^{M_A} \ell_j^{(A)}(\theta)\Phi_j^{(A)}, && \theta \in [-h, -\bar{a}_A],\\
Q_{M_J}^{(J)}(\theta) &= \sum_{j=0}^{M_J} \ell_j^{(J)}(\theta)\Psi_j^{(J)}, && \theta \in [-\bar{a}_A, 0],\\
Q_{M_A}^{(A)}(\theta) &= \ell_0^{(A)}(\theta)\Psi_{M_J}^{(J)} + \sum_{j=1}^{M_A} \ell_j^{(A)}(\theta)\Psi_j^{(A)}, && \theta \in [-h, -\bar{a}_A].
\end{aligned}$$

The unknown value $P_{M_J}^{(J)}(\theta_0^{(J)}) = P_M(\theta_0^{(J)})$ is determined as a linear function of (Φ, Ψ) by virtue of (2.1) and of (3.8)–(3.9):

$$\begin{aligned}
P_{M_J}^{(J)}(\theta_0^{(J)}) = {} & w_0^{(A)} \left[\tilde{B}_{11}^{(A)}(\theta_0^{(A)})\Phi_{M_J}^{(J)} + \tilde{B}_{12}^{(A)}(\theta_0^{(A)})\Psi_{M_J}^{(J)}\right]\\
& + \tilde{A}_{12}\Psi_0^{(J)} + \sum_{k=0}^{M_J} w_k^{(J)} \tilde{B}_{12}^{(J)}(\theta_k^{(J)})\Psi_k^{(J)}\\
& + \sum_{k=1}^{M_A} w_k^{(A)} \left[\tilde{B}_{11}^{(A)}(\theta_k^{(A)})\Phi_k^{(A)} + \tilde{B}_{12}^{(A)}(\theta_k^{(A)})\Psi_k^{(A)}\right].
\end{aligned} \tag{3.10}$$

This leads (P_M, Q_M) to be an explicit linear function of (Φ, Ψ). The matrix $\mathcal{A}_M$ is obtained by following (2.5)–(2.7). Below we use the coefficients

$$d_{ij}^{(*)} := \ell_j'(\theta_i^{(*)}), \qquad i = 1, \ldots, M_*,\ j = 0, 1, \ldots, M_*,$$

which are the elements of the Chebyshev differentiation matrices relevant to (3.6)–(3.7) for $* = J, A$. These matrices can be efficiently computed as explained in [32]. With reference to the resulting structure of $\mathcal{A}_M$ depicted in Figure 1, the first block from the top accounts for the exact differentiation of $P_{M_J}^{(J)}$ at the nodes of (3.6) excluded $\theta_0^{(J)} = 0$. It is the analogue of (2.5) restricted to $[-\bar{a}_A, 0]$, but now all the components of (Φ, Ψ) contribute by (3.10), hence the size is $M_J \times (2M + 1)$ and the entries are

$$(\mathcal{A}_M)_{i,j} = \begin{cases} d_{ij}^{(J)}, & j = 1, \ldots, M_J - 1, \\ d_{iM_J}^{(J)} + d_{i0}^{(J)} w_0^{(A)} \tilde{B}_{11}^{(A)}(\theta_0^{(A)}), & j = M_J, \\ d_{i0}^{(J)} w_k^{(A)} \tilde{B}_{11}^{(A)}(\theta_k^{(A)}), & j = M_J + k,\ k = 1 \ldots, M_A, \\ d_{i0}^{(J)} \left[\tilde{A}_{12} + w_0^{(J)} \tilde{B}_{12}^{(J)}(\theta_0^{(J)}) \right], & j = M + 1, \\ d_{i0}^{(J)} w_k^{(J)} \tilde{B}_{12}^{(J)}(\theta_k^{(J)}), & j = M + 1 + k,\ k = 1, \ldots, M_J - 1, \\ d_{i0}^{(J)} \left[w_{M_J}^{(J)} \tilde{B}_{12}^{(J)}(\theta_{M_J}^{(J)}) + w_0^{(A)} \tilde{B}_{12}^{(A)}(\theta_0^{(A)}) \right], & j = M + 1 + M_J, \\ d_{i0}^{(J)} w_k^{(A)} \tilde{B}_{12}^{(A)}(\theta_k^{(A)}), & j = M + 1 + M_J + k,\ k = 1, \ldots, M_A, \end{cases}$$

for $i = 1, \ldots, M_J$. The second block from the top in Figure 1 accounts for the exact differentiation of $P_{M_A}^{(A)}$ at the nodes of (3.7) excluding $\theta_0^{(A)} = -\bar{a}_A = \theta_{M_J}^{(J)}$. It is the analogue of (2.5) restricted to $[-h, -\bar{a}_A]$, with size $M_A \times (M_A + 1))$ and entries

$$(\mathcal{A}_M)_{M_J+i, M_J+j} = d_{ij}^{(A)}, \qquad i = 1, \ldots, M_A,\ j = 0, 1, \ldots, M_A.$$

The third block from the top in Figure 1 accounts for the exact differentiation of $Q_{M_J}^{(J)}$ at $\theta_0^{(J)}$. It is the analogue of (2.6) since $Q_M(\theta_0^{(J)}) = Q_{M_J}^{(J)}(\theta_0^{(J)})$, but again all the components of (Φ, Ψ) contribute by (3.10), hence the size is $1 \times (2M + 1)$ and the entries are

$$(\mathcal{A}_M)_{M+1,j} = \begin{cases} w_k^{(J)} \tilde{B}_{21}^{(J)}(\theta_k^{(J)}), & j = k,\ k = 1, \ldots, M_J - 1, \\ w_0^{(A)} \left[\tilde{B}_{21}^{(A)}(\theta_0^{(A)}) + e_0^{(J)} \tilde{B}_{11}^{(A)}(\theta_0^{(A)}) \right] + w_{M_J}^{(J)} \tilde{B}_{21}^{(J)}(\theta_{M_J}^{(J)}), & j = M_J, \\ w_k^{(A)} \left[\tilde{B}_{21}^{(A)}(\theta_k^{(A)}) + e_0^{(J)} \tilde{B}_{11}^{(A)}(\theta_k^{(A)}) \right], & j = M_J + k,\ k = 1 \ldots, M_A, \\ \tilde{A}_{22} + e_0^{(J)} \tilde{A}_{12} + w_0^{(J)} \left[\tilde{B}_{22}^{(J)}(\theta_0^{(J)}) + e_0^{(J)} \tilde{B}_{12}^{(J)}(\theta_0^{(J)}) \right], & j = M + 1, \\ w_k^{(J)} \left[\tilde{B}_{22}^{(J)}(\theta_k^{(J)}) + e_0^{(J)} \tilde{B}_{12}^{(J)}(\theta_k^{(J)}) \right], & j = M + 1 + k, \\ & k = 1, \ldots, M_J - 1, \\ w_{M_J}^{(J)} \left[\tilde{B}_{22}^{(J)}(\theta_{M_J}^{(J)}) + e_0^{(J)} \tilde{B}_{12}^{(J)}(\theta_{M_J}^{(J)}) \right] & \\ \quad + w_0^{(A)} \left[\tilde{B}_{22}^{(A)}(\theta_0^{(A)}) + e_0^{(J)} \tilde{B}_{12}^{(A)}(\theta_0^{(A)}) \right], & j = M + 1 + M_J, \\ w_k^{(A)} \left[\tilde{B}_{22}^{(A)}(\theta_k^{(A)}) + e_0^{(J)} \tilde{B}_{12}^{(A)}(\theta_k^{(A)}) \right], & j = M + 1 + M_J + k, \\ & k = 1, \ldots, M_A, \end{cases}$$

where we set $e_0^{(J)} := w_0^{(J)} \tilde{B}_{21}^{(J)}(\theta_0^{(J)})$ for brevity. The fourth block from the top in Figure 1 accounts for the exact differentiation of $Q_{M_J}^{(J)}$ at the nodes of (3.6) excluding

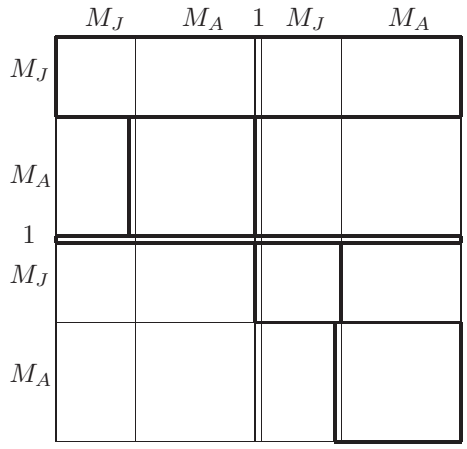

FIG. 1. *Block structure (thick) and sizes (thin) of $\mathcal{A}_M$ for Daphnia models.*

$\theta_0^{(J)} = 0$. It is the analogue of (2.7) restricted to $[-\bar{a}_A, 0]$, with size $M_J \times (M_J + 1)$ and entries

$$(\mathcal{A}_M)_{M+1+i,M+1+j} = d_{ij}^{(J)}, \qquad i = 1, \dots, M_J,\ j = 0, 1, \dots, M_J.$$

The fifth block from the top in Figure 1 accounts for the exact differentiation of $Q_{M_A}^{(A)}$ at the nodes of (3.7) excluding $\theta_0^{(A)} = -\bar{a}_A = \theta_{M_J}^{(J)}$. It is the analogue of (2.7) restricted to $[-h, -\bar{a}_A]$, the size is $M_A \times (M_A + 1)$, and the entries are

$$(\mathcal{A}_M)_{M+1+M_J+i,M+1+M_J+j} = d_{ij}^{(A)}, \qquad i = 1, \dots, M_A,\ j = 0, 1, \dots, M_A.$$

The remaining part of $\mathcal{A}_M$ has zero entries. Eventually, notice the considerable cost reduction thanks to the choice made in the previous section, since there is no need to construct and evaluate Lagrange coefficients, as would be the case if we used a nonpiecewise polynomial.

Remark 3.1. The arguments illustrated in sections 3.1 and 3.2 can be extended to systems of linear VFEs/DDEs (1.13) where the generic exact linear functional (1.17) contains p discrete and distributed delay terms, i.e.,

$$L(\phi, \psi) = \sum_{k=0}^{p} A^{(k)}(\phi, \psi)(-\tau_k) + \sum_{k=1}^{p} \int_{-\tau_k}^{-\tau_{k-1}} B^{(k)}(\theta)(\phi, \psi)(\theta) d\theta$$

for given delays $0 =: \tau_0 < \tau_1 < \cdots < \tau_p := \tau$, given matrices $A^{(k)} \in \mathbb{R}^{d \times d}$ for $k = 0, 1, \dots, p$, and given sufficiently smooth matrix functions $B^{(k)} : [-\tau_k, -\tau_{k-1}] \to \mathbb{R}^{d \times d}$ for $k = 1, \dots, p$, where $d = d_1 + d_2$. This extension does not introduce any theoretical difficulty. Indeed, the convergence analysis of section 2.1 also applies with minor and obvious modifications (see, e.g., [7, section 5.4] for DDEs). In contrast, major technicalities are the price to pay in terms of indexing w.r.t. number of equations and delays. For this reason we avoid such generality in the present work. Nevertheless, the MATLAB codes available from the authors are written in this more (and most) general setting.

To complete the construction of $\mathcal{A}_M$ it is necessary to compute the A's and B's through the relevant approximations $\tilde{A}$'s and $\tilde{B}$'s. Note that the values of the $\tilde{B}$'s are required only at the mesh nodes. This is the argument of the forthcoming sections.

3.3. Numerical solution of ODEs. To address the above task one would require the knowledge of $X(\cdot,\bar{S})$ and $\mathcal{F}(\cdot,\bar{S})$ on $[0,h]$ (recall the notation introduced for (1.11)–(1.12)). In practice, we need the values corresponding at minus the mesh nodes in (3.6)–(3.7), e.g., for $B_{11}^{(A)}$, and, in principle, at any other point of $[0,h]$ for the inner integrals. Indeed, even if the latter are approximated by quadrature, it is rather difficult to know in advance the quadrature nodes, as explained next in section 3.4.

In [11], (1.2)–(1.3) are solved numerically for computing the equilibria $(\bar{b},\bar{S})$ by using DOPRI5. It is an embedded Runge–Kutta pair with dense output, event location, and variable stepsize to control the error [19, 26]. Dense output means that the numerical solution is available at any point of the integration window within a given tolerance and a uniform convergence order. The variable stepsize control strategy guarantees either a prescribed absolute tolerance TOL_a and a relative one TOL_r. The uniform order is 4. Dense output is mandatory here since the points of evaluations of $X(\cdot,\bar{S})$ and $\mathcal{F}(\cdot,\bar{S})$ are, in general and as explained above, different from the nodes of the used Runge–Kutta mesh (also because the stepsize is variable). Moreover, dense output allows for event location, necessary to compute the maturation age $\bar{a}_A$ through $X(\bar{a}_A,\bar{S})=x_A$. The latter is solved by substituting X with the numerical dense solution $\tilde{X}$ and by solving $\tilde{X}(\bar{a}_A,\bar{S})-x_A=0$ through, e.g., Netwon-like methods.

For all these reasons, in this work we apply DOPRI5 and we use a Broyden method [8] for the maturation age. Everything is implemented in the MATLAB codes available by the authors.

3.4. Quadrature of inner integrals. The lack of an analytical expression of $X(\cdot,\bar{S})$ and $\mathcal{F}(\cdot,\bar{S})$ for what was seen in the previous section imposes the numerical quadrature of the inner integrals. To this aim we adopt the same Clenshaw–Curtis formula illustrated in section 3.1.

There are different intervals of integration involved in the A's and B's. Also, many of them vary with $\theta\in\Omega_{M_*}^*$, $*=J,A$. As a further complication, the integrands (or their derivatives) have possible discontinuities when juveniles become adults. This is due, e.g., to the presence of $\mathcal{K}(\alpha_1,\alpha_2)$ given in (1.6) and of $\mathcal{H}(\alpha_1,\alpha_2)$ given in (1.7), which can be discontinuous at $\alpha_2=\bar{a}_A$. As a consequence, to guarantee convergence and a spectrally accurate error (as discussed at the end of section 3.1), we use a piecewise quadrature whenever $\bar{a}_A$ belongs to the integration interval.

As an example, consider the second term in the last integral in $B_{22}^{(J)}$. All the other inner integrals in the A's and B's are treated analogously. The discretization of the infinitesimal generator requires the evaluation of

$$I_i := \int_{-\theta_i^{(J)}}^{h} \gamma(\sigma)\mathcal{H}(\sigma,\sigma+\theta_i^{(J)})d\sigma, \qquad i=0,1,\dots,M_J.$$

Recall first that $\gamma(\sigma)=\gamma(X(\sigma,\bar{S}),\bar{S})$ can be discontinuous across the maturation size x_A, i.e., at $\sigma=\bar{a}_A$. We call $\gamma^{(J)}$ the restriction of γ relevant to $X\in[x_b,x_A]$, i.e., $\sigma\in[0,\bar{a}_A]$, and $\gamma^{(A)}$ the restriction of γ relevant to $X\in[x_A,x_{\max}]$, i.e., $\sigma\in[\bar{a}_A,h]$, where $x_{\max}$ is the maximum size reached by the adults. Notice that X is continuous as solution of (1.2). Second, from (1.7), we know that $\mathcal{H}$ is discontinuous at $\bar{a}_A$ in the second argument, since so are $\mathcal{K}$ in (1.6) and μ_2 (for the same reasoning of γ above, which holds for g_2 in (1.6), too). This affects the integrand whenever $\sigma=\bar{a}_A-\theta_i^{(J)}$.

Accordingly and recalling that $-\theta_i^{(J)} \le \bar{a}_A$, we split the integral as

$$I_i = \int_{-\theta_i^{(J)}}^{\bar{a}_A} \gamma^{(J)}(\sigma)\mathcal{H}^{(J)}(\sigma,\sigma+\theta_i^{(J)})d\sigma + \int_{\bar{a}_A}^{\bar{a}_A-\theta_i^{(J)}} \gamma^{(A)}(\sigma)\mathcal{H}^{(J)}(\sigma,\sigma+\theta_i^{(J)})d\sigma + \int_{\bar{a}_A-\theta_i^{(J)}}^{h} \gamma^{(A)}(\sigma)\mathcal{H}^{(A)}(\sigma,\sigma+\theta_i^{(J)})d\sigma$$

for $i = 0, 1, \ldots, \bar{i}$ and

$$I_i = \int_{-\theta_i^{(J)}}^{\bar{a}_A} \gamma^{(J)}(\sigma)\mathcal{H}^{(J)}(\sigma,\sigma+\theta_i^{(J)})d\sigma + \int_{\bar{a}_A}^{h} \gamma^{(A)}(\sigma)\mathcal{H}^{(J)}(\sigma,\sigma+\theta_i^{(J)})d\sigma$$

for $i = \bar{i}+1, \ldots, M_J$, where $\bar{i} := \max\{i \ : \ \bar{a}_A - \theta_i^{(J)} \le h\}$. Then (3.5) is applied separately to each one of the integrals above.

To conclude, we observe that, due to convergence considerations, it would be appropriate to choose different quadrature degrees n, mainly depending on the length of the integration intervals. Standard error estimates [33] require the knowledge of bounds on high-order derivatives of the integrands, which, in our case, differ from term to term and, above all, are only numerically available. Extending the argument also to all the other integrals in the A's and B's makes it unattainable. Therefore, we choose to fix n in advance (and independently of M) for all the inner quadratures, taking into account that spectral convergence guarantees in general high accuracy with rather low n (e.g., $n \le 20$; see also section 4).

4. Numerical results. We consider the Daphnia model in [11, section 4.1]. Vital rates and relevant parameters are listed in Table 1.

TABLE 1
Rates (top) and parameters (bottom) of the considered Daphnia model.

resource intrinsic rate of change	$f(S) = a_1 S(1 - S/C)$
consumer growth rate	$g(x,S) = \gamma_g\,(x_m f_r(S) - x)$
consumer mortality rate	$\mu(x,S) = \mu$
consumer adults reproduction rate	$\beta(x,S) = r_m f_r(S) x^2$
consumer ingestion rate	$\gamma(x,S) = \nu_S f_r(S) x^2$
Holling type II functional response	$f_r(S) := \xi S/(1+\xi S)$
size at birth	$x_b = 0.8$
size at maturation	$x_A = 2.5$
maximum size	$x_m = 6.0$
growth time constant	$\gamma_g = 0.15$
functional response shape parameter	$\xi = 7.0$
maximum feeding rate	$\nu_S = 1.8$
maximum reproduction rate	$r_m = 0.1$
mortality rate parameter	$\mu =$ varying
environment carrying capacity	$C =$ varying
flow-through rate	$a_1 = 0.5$
maximum age	$h = 70$

First we test the convergence of the computed eigenvalues, in particular, the overall spectral accuracy of Theorem 2.6 and how the different error sources affect the approximation through the term ε in (2.12). We recall that the final accuracy depends on the main index M relevant to the discretization mesh (sections 3.1 and 3.2), on the absolute and relative tolerances of the DOPRI5 method, respectively, TOL_a and TOL_r (section 3.3), and on the degree n of the quadrature of the inner integrals

(section 3.4). The experiments refer to the computation of the rightmost eigenvalue of the positive equilibrium $(\bar{b}, \bar{S}) = (0.003833012934926, 0.351318582230538)$ for $\mu = 0.243845788916114$ and $C = 0.887255640320707$. We consider as exact this eigenvalue computed with $M = 500$, $\mathrm{TOL}_a = 10^{-14}$, $\mathrm{TOL}_r = 10^{-8}$, and $n = 100$. We compare the trends of the error obtained by increasing M from 10 to 50 and by keeping all the other numerical parameters as fixed except for one. The results are collected in Figure 2: top panel for varying TOL_a, middle panel for varying TOL_r, and bottom panel for varying n. Theorem 2.6 is confirmed in all panels: the error decays following spectral accuracy $O(M^{-M})$ down to a barrier which is due to the term ε in (2.12). In the top and middle panels, respectively, we see that TOL_a does not affect the error, whereas TOL_r does. Clearly, the barrier lowers as the relative resolution of DOPRI5 increases. In the bottom panel we see that the barrier decreases as n increases but, beyond $n = 20$, we do not appreciate further advantages (as discussed at the end of section 3.4). Finally, we remark that the lowest barrier around 10^{-10} may be due to machine round-off: indeed, during the computations we noticed an instability phenomenon similar to the one explained in [34]. We may further investigate this subject in the future and, in this respect, also the study of the (non) normality of the matrix $\mathcal{A}_M$ appears to be an important question [29, 31].

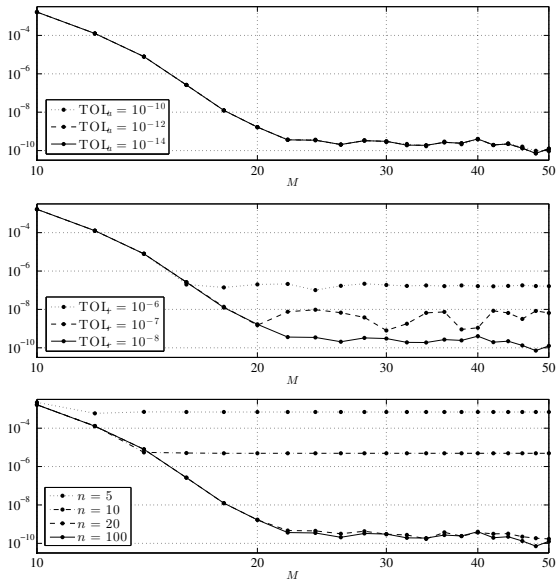

FIG. 2. *Convergence of the error of the rightmost eigenvalue; see text.*

Now we compute the eigenvalues for several choices of the mortality μ and of the carrying capacity C in the (μ, C)-parameter plane. The aim is to check the correctness of the transcritical and Hopf bifurcation curves computed in [11, Figure 7], there called respectively *existence* and *stability* boundaries. Below the existence boundary only the trivial equilibrium exists and it is stable. Above it loses stability in favor of the existing positive equilibrium. Therefore, the existence boundary is determined by analyzing the position w.r.t. the imaginary axis of the rightmost eigenvalue of the trivial equilibrium. The stability boundary, instead, is determined by analyzing the position w.r.t. the imaginary axis of the rightmost eigenvalue of the positive

equilibrium (a complex-conjugate pair): below the boundary the latter is stable, above it is unstable. Such boundaries, obtained with the method in [11] based on the use of the characteristic equation as discussed at the end of section 1.2, are shown in Figures 3 and 4. Figure 3 includes a number of rightmost eigenvalues of the trivial equilibrium computed with the method proposed in this work for several values of μ and C corresponding to the points $*$ in the top panel. The series of panels (a)–(c) and (d)–(f) confirm the transcritical bifurcation from the trivial equilibrium to the positive one. Similar computations are shown in Figure 4 for the nontrivial equilibrium and its stability boundary: the series of panels (a)–(c) and (d)–(f) confirm the Hopf bifurcation of the positive equilibrium. Notice how in both cases the computation of the eigenvalues allows us to appreciate the positive crossing speed at the bifurcation points.

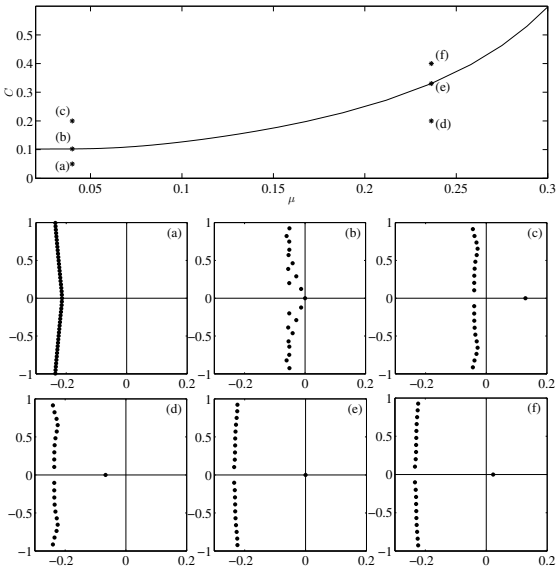

FIG. 3. *Existence boundary in the* (μ, C)*-parameter plane (top panel); eigenvalues of the trivial equilibrium corresponding to points* $*$ *in the top panel (panels* (a)–(f)*): relevant parameter values at machine precision are* $\mu = 0.040030019682702$ (a)–(c) *and* 0.236338384280189 (d)–(f) *and* $C = 0.05$ (a)*,* 0.102409511357698 (b)*,* 0.2 (c)–(d)*,* 0.330235018740724 (e)*, and* 0.4 (f)*.*

Appendix A. As motivated in [16], by the implicit function theorem the equation $x(\tau; a, \psi) = x_A$ has for $a > \bar{a}_A$ and ψ close to $\bar{S}$ a solution $\tilde{\tau}(a, \psi)$ (note that $\bar{a}_A = \tilde{\tau}(a, \bar{S})$ independently of a). Then we can rewrite (1.2) as

$$x(\tau) = x_b + \int_0^\tau g(x(\sigma), \psi(-a + \sigma))d\sigma, \qquad \tau \in [0, \tilde{\tau}(a, \psi)). \tag{A.1}$$

With the shorthand notation $\varkappa(\tau) = \varkappa(\tau; a, \bar{S}, \psi) := D_3 x(\tau; a, \bar{S})\psi$, we get

$$\varkappa(\tau) = \int_0^\tau \left[g_1(\sigma)\varkappa(\sigma) + g_2(\sigma)\psi(-a + \sigma)\right] d\sigma, \qquad \tau \in [0, \bar{a}_A),$$

or, alternatively,

$$\varkappa'(\tau) = g_1(\tau)\varkappa(\tau) + g_2(\tau)\psi(-a + \tau), \qquad \tau \in (0, \bar{a}_A), \tag{A.2}$$

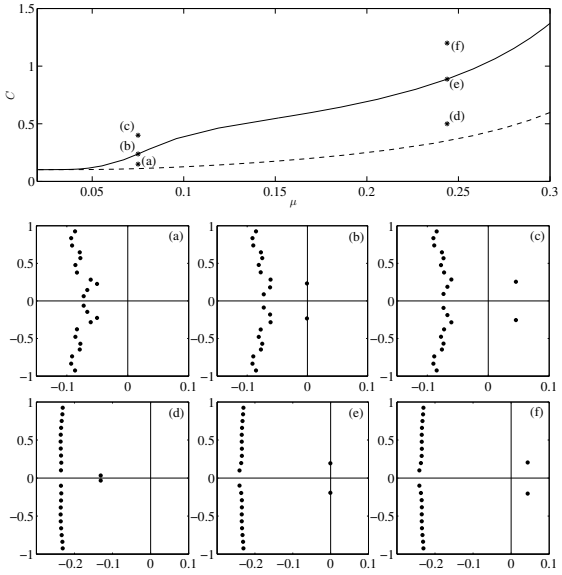

FIG. 4. *Existence (dashed) and stability (solid) boundaries in the* (μ, C)*-parameter plane (top panel); eigenvalues of the nontrivial equilibrium corresponding to points* $*$ *in the top panel (panels* (a)–(f)*): relevant parameter values at machine precision are* $\mu = 0.075058160583520$ (a)–(c) *and* 0.243845788916114 (d)–(f) *and* $C = 0.15$ (a), 0.237850694572043 (b), 0.4 (c), 0.5 (d), 0.887255640320707 (e), *and* 1.2 (f).

with $\varkappa(0) = 0$, which yields

$$\varkappa(\tau) = \int_0^\tau \mathcal{K}(\tau, \alpha)\psi(-a + \alpha)d\alpha$$

through (1.6). For $\tau > \tilde{\tau}(a, \psi)$ we consider instead

$$x(\tau) = x_A + \int_{\tilde{\tau}(a,\psi)}^\tau g(x(\sigma), \psi(-a + \sigma))d\sigma. \tag{A.3}$$

If we differentiate (A.1) in ψ for $\tau \uparrow \tilde{\tau}(a, \psi)$ we get

$$D_2\tilde{\tau}(a, \bar{S})\psi = -\frac{\varkappa^-(\bar{a}_A)}{g^-} = -\frac{1}{g^-}\int_0^{\bar{a}_A} \mathcal{K}(\bar{a}_A, \alpha)\psi(-a + \alpha)d\alpha. \tag{A.4}$$

By using the latter we can differentiate (A.3) to get

$$\varkappa(\tau) = \frac{g^+}{g^-}\varkappa^-(\bar{a}_A) + \int_{\bar{a}_A}^\tau \left[g_1(\sigma)\varkappa(\sigma) + g_2(\sigma)\psi(-a + \sigma)\right] d\sigma$$

for $\tau > \bar{a}_A$ or, alternatively, (A.2) for $\tau > \bar{a}_A$ with initial condition

$$\varkappa^+(\bar{a}_A) = \frac{g^+}{g^-}\varkappa^-(\bar{a}_A). \tag{A.5}$$

Application of the variation of constants formula to the latter initial value problem yields that for any $\tau \leq a$ we get

$$\begin{aligned} D_3x(\tau;a,\bar{S})\psi &= \varkappa(\tau) \\ &= \int_0^\tau \mathcal{K}(\tau,\alpha)\psi(-a+\alpha)d\alpha \\ &\quad +H(\tau-\bar{a}_A)\left(\frac{g^+}{g^-}-1\right)\int_0^{\bar{a}_A}\mathcal{K}(\tau,\alpha)\psi(-a+\alpha)d\alpha. \end{aligned} \tag{A.6}$$

Note that, vice versa, $\varkappa$ satisfies (A.2) for all $\tau \in (0,\bar{a}_A)\cup(\bar{a}_A,a)$ together with (A.5), which shows its correctness. Essentially the same method applied to (1.3) and using (A.6) yields

$$\begin{aligned} D_3\bar{\mathcal{F}}(\tau;a,\bar{S})\psi &= \int_0^\tau \mathcal{H}(\tau,\alpha)\psi(-a+\alpha)d\alpha \\ &\quad +H(\tau-\bar{a}_A)\mathcal{F}(\tau,\bar{S})\left[\frac{\mu^- - \mu^+}{g^-}\int_0^{\bar{a}_A}\mathcal{K}(\bar{a}_A,\alpha)\psi(-a+\alpha)d\alpha\right. \\ &\quad \left. -\left(\frac{g^+}{g^-}-1\right)\int_0^{\bar{a}_A}\left(\int_{\bar{a}_A}^\tau \mu_1(\sigma)\mathcal{K}(\sigma,\alpha)d\sigma\right)\psi(-a+\alpha)d\alpha\right] \end{aligned}$$

(and shows its correctness). Eventually, by defining $D_2X(a,\bar{S})\psi := D_3x(a;a,\bar{S})\psi$ and $D_2\mathcal{F}(a,\bar{S})\psi := D_3\bar{\mathcal{F}}(a;a,\bar{S})\psi$ and setting $a=\bar{a}_A$ in (A.4) we obtain (1.8)–(1.10).

Acknowledgment. We thank Odo Diekmann for fruitful discussions on, among others, the derivation of the characteristic equation.

REFERENCES

[1] E. L. Allgower and K. Georg, *Introduction to Numerical Continuation Methods*, Classics in Appl. Math. 45, SIAM, Philadelphia, 2003.

[2] J. Boyd, *Chebyshev and Fourier Spectral Methods*, 2nd ed., Dover, New York, 2001.

[3] D. Breda, O. Diekmann, S. Maset, and R. Vermiglio, *A numerical approach for investigating the stability of equilibria for structured population models*, J. Biol. Dyn., 7 (2013), pp. 4–20.

[4] D. Breda, S. Maset, and R. Vermiglio, *Pseudospectral differencing methods for characteristic roots of delay differential equations*, SIAM J. Sci. Comput., 27 (2005), pp. 482–495.

[5] D. Breda, S. Maset, and R. Vermiglio, *Pseudospectral approximation of eigenvalues of derivative operators with non-local boundary conditions*, Appl. Numer. Math., 56 (2006), pp. 318–331.

[6] D. Breda, S. Maset, and R. Vermiglio, *Numerical recipes for investigating endemic equilibria of age-structured SIR epidemics*, Discrete Contin. Dyn. Syst. Ser. A, 32 (2012), pp. 2675–2699.

[7] D. Breda, S. Maset, and R. Vermiglio, *Stability of Linear Delay Differential Equations: A Numerical Approach with MATLAB*, Springer Briefs Control Automation Robotics, Springer, New York, 2015.

[8] C. G. Broyden, *A class of methods for solving nonlinear simultaneous equations*, Math. Comp., 19 (1965), pp. 577–593.

[9] J. B. Conway, *Functions of One Complex Variable*, 2nd ed., Grad. Texts in Math. 11, Springer, New York, 1978.

[10] A. M. de Roos, *A gentle introduction to models of physiologically structured populations*, in Structured-Population Models in Marine, Terrestrial and Freshwater Systems, S. Tuljapurkar and H. Caswell, eds., Chapman and Hall, New York, 1997, pp. 119–204.

[11] A. M. de Roos, O. Diekmann, P. Getto, and M. A. Kirkilionis, *Numerical equilibrium analysis for structured consumer resource models*, Bull. Math. Biol., 72 (2010), pp. 259–297.

[12] A. M. de Roos, J. A. J. Metz, E. Evers, and A. Leipoldt, *A size-dependent predator prey interaction: Who pursues whom?*, J. Math. Biol., 28 (1990), pp. 609–643.
[13] A. M. de Roos and L. Persson, *Population and Community Ecology of Ontogenetic Development*, Monogr. Population Biology 51, Princeton University Press, Princeton, NJ, 2013.
[14] O. Diekmann, P. Getto, and M. Gyllenberg, *Stability and bifurcation analysis of Volterra functional equations in the light of suns and stars*, SIAM J. Math. Anal., 39 (2007), pp. 1023–1069.
[15] O. Diekmann, M. Gyllenberg, J. A. J. Metz, S. Nakaoka, and A. M. de Roos, *Corrigendum to "Daphnia revisited: Local stability and bifurcation theory for physiologically structured population models explained by way of an example,"* in preparation.
[16] O. Diekmann, M. Gyllenberg, J. A. J. Metz, S. Nakaoka, and A. M. de Roos, *Daphnia revisited: Local stability and bifurcation theory for physiologically structured population models explained by way of an example*, J. Math. Biol., 61 (2010), pp. 277–318.
[17] O. Diekmann and K. Korvasová, *Linearization of solution operators for state-dependent delay equations: A simple example*, Discrete Contin. Dyn. Syst. Ser. A, 36 (2016), pp. 137–149.
[18] O. Diekmann, S. A. van Gils, S. M. Verduyn Lunel, and H. O. Walther, *Delay Equations: Functional, Complex and Nonlinear Analysis*, Appl. Math. Sci. 110, Springer, New York, 1995.
[19] J. R. Dormand and P. J. Prince, *A family of embedded runge-kutta formulae*, J. Comput. Appl. Math., 6 (1980), pp. 19–26.
[20] K. Engel and R. Nagel, *One-Parameter Semigroups for Linear Evolution Equations*, Grad. Texts in Math. 194, Springer, New York, 1999.
[21] C. I. Gheorghiu, *Spectral Methods for Non-Standard Eigenvalue Problems: Fluid and Structural Mechanics and Beyond*, Springer Briefs in Math., Springer, New York, 2014.
[22] J. K. Hale and S. M. Verduyn Lunel, *Introduction to Functional Differential Equations*, 2nd ed., Appl. Math. Sci. 99, Springer, New York, 1993.
[23] N. Krasovskii, *Stability of Motion*, Stanford University Press, Stanford, CA, 1963.
[24] R. Kress, *Linear Integral Equations*, Appl. Math. Sci. 82, Springer, New York, 1989.
[25] V. I. Krylov, *Convergence of algebraic interpolation with respect to roots of Chebyshev's polynomial for absolutely continuous functions of bounded variation*, Dokl. Akad. Nauk SSSR, 107 (1956), pp. 362–365.
[26] B. Owren and M. Zennaro, *Continuous explicit Runge-Kutta methods*, in Computational Ordinary Differential Equations (London, 1989), I. R. Cash and I. Gladwell, eds., Inst. Math. Appl. Conf. Ser. 39, Oxford University Press, New York, 1992, pp. 97–105.
[27] F. Scarabel, *Numerical Methods to Study the Dynamics of Retarded Functional Differential Equations*, Master's thesis, University of Udine, 2013.
[28] H. Sleijpen and G. Van der Vorst, *A Jacobi-Davidson iteration method for linear eigenvalue problems*, SIAM Rev., 42 (2000), pp. 267–293.
[29] D. M. Sloan, *On the norms of inverses of pseudospectral differentiation matrices*, SIAM J. Numer. Anal., 42 (2004), pp. 30–48.
[30] H. L. Smith, *An Introduction to Delay Differential Equations with Applications to the Life Sciences*, Texts in Appl. Math. 57, Springer, New York, 2011.
[31] L. N. Trefethen, *Computation of pseudospectra*, Acta Numer., 8 (1999), pp. 1–110.
[32] L. N. Trefethen, *Spectral methods in MATLAB*, Software Environ. Tools, SIAM, Philadelphia, 2000.
[33] L. N. Trefethen, *Is Gauss quadrature better than Clenshaw–Curtis?*, SIAM Rev., 50 (2008), pp. 67–87.
[34] L. N. Trefethen and M. R. Trummer, *An instability phenomenon in spectral methods*, SIAM J. Numer. Anal, 24 (1987), pp. 1008–1023.